Operational modeling issues in extreme weather coastal flooding

Diana Di Luccio[1] (*diana.diluccio@uniparthenope.it*),
Luigi Mucerino[4] (*luigi.mucerino@edu.unige.it*),
Guido Benassai[2] (*guido.benassai@uniparthenope.it*),
Giorgio Budillon[1] (*giorgio.budillon@uniparthenope.it*),
Raffaele Montella[1] (*raffaele.montella@uniparthenope.it*),
Eugenio Pugliese Carratelli[3] (*epc@unisa.it*),
Ferdinando Reale[3] (*freale@unisa.it*),
Fabio Dentale[3] (*fdentale@unisa.it*)

[1] *University of Naples "Parthenope", Science and Technologies Department, Centro Direzionale Is. C4, 80143 Napoli, Italy*

[2]*University of Naples "Parthenope", Engineering Department, Centro Direzionale Is. C4, 80143 Napoli, Italy*

[3]*Inter-University Consortium for the Prediction and Prevention of Major Risks Hazards (CUGRI), 84080 Penta di Fisciano (SA), Italy*

[4]*University of Genova, Department of Earth, Environment and Life Sciences, Corso Europa 26, 16132 Genova, Italy*

Abstract. The coastal environment is a highly complex dynamic system, influenced by natural and human factors contributing to its spatial and temporal evolution. The Italian coasts are heavily affected by human activities and extreme weather/marine events could generate extensive landscape, social and economic damage.

The goal of this paper is to provide and to test an operational system based on coupled atmospheric and marine numerical models with the aim to perform accurate forecasts and to manage the potential hazards for citizens, infrastructures, properties, wildlife and coastal ecosystems impacted by extreme storms. We developed an operational alert system configured for each point of interest applying rules fed by the local high resolution forecasted data. The alert system sends warnings to the users in case of coastal flooding.

The project scientific and technological results could be considered in order to provide a decision support to local authorities and beach resort companies in case of extreme sea storm events. The system reliability is demonstrated comparing the model produced forecasts with buoys recorded data, satellite observations and video camera images processing.

Keywords: *scientific workflow; waves; forecasting model; coastal flooding; video monitoring; beach.*

1. Introduction

The impact of climate changes along the coastal regions may include the presence of events that severely affect the Earth system dynamics, such as the possible increase of sea surface temperatures as well as the changes in frequency, intensity and duration of wave storms (Giarrusso et al. 1999, Carratelli et al. 2007a, Benassai et al. 2015).

Sea waves, whether driven by local winds or swell, can cause coastal flooding; its extent, which is a function of the elevation, is controlled by the topography of the coastal land and by the possible presence of coastal protection structures. The operational modeling of wave climate and particularly of extreme storms is indeed one of the most challenging activities of modern oceanography: a number of Authors are thus developing this activity in order to provide forecast information of many extreme sea storms potential effects (beach and dune erosion, overwash, inundation, etc.) which can be accompanied by infrastructures damage and citizen danger (Mendoza et al. 2004, Sartini et al. 2016).

The verification of the wave numerical model results has been made by a number of authors, with regard to both the sea wave height and wave spectra and to some global parameters influencing coastal vulnerability (Benassai et al. 2013) such as the beach retreat and inundation distance.

These comparisons have been made with reference to in situ wave measurements and satellite observations obtained by altimeter (Carratelli et al. 2006, Reale et al. 2013) and *Synthetic Aperture Radar* (SAR) platforms (Benassai et al. 2013, Carratelli et al. 2007).

The availability of low-cost beach video monitoring systems produced a good amount of wave storm images which have been used to extract beach run-up and associated flooding distance.

The run-up forecasting can be used to provide a decision support to local Authorities and useful hazard information for citizens.

In this context, the paper describes a scientific workflow implemented in order to forecast and to manage the potential hazard due to coastal flooding. The objectives are achieved by making the use of a high spatial resolution weather-ocean forecasting system implemented by *Campania Center for Marine and Atmospheric Monitoring and Modelling* (CCMMMA) - University of Naples "*Parthenope*", using a high performance computing (HPC) system for simulation and open environmental data dissemination (Montella et al. 2007). The numerical models (Giunta et al. 2005), with a specific parameterization and spatial/temporal resolution, have been integrated in *Framework to Advance Climate, Economic, and Impact Investigations with Information Technology* (Face-IT) (Foster et al. 2013) workflow system. The models which compose the scientific workflow (Pham et al. 2012) are actually operative and the data are free available at *meteo.uniparthenope.it*.

In detail, the deep water numerical models are integrated with a wave propagation model in shallow water and the consequent run-up evaluation on the beach.

The simulations have been compared with beach video camera acquisitions during the wave storms.

The paper is organized as follows: the scientific workflow description and the testing dataset are reported in chapter 2, the numerical results and the comparison with observations are given in chapters 3, 4 and 5, and finally, the conclusion and the future directions are reported in chapter 6.

2. Theoretical and technical background

In this paragraph, the components which are parts of the implemented scientific workflow and the dataset used to test the performances of the operational system are presented.

2.1 Tools and scientific workflow

The weather/sea forecasting tool in Fig. 1 has been configured using an HPC infrastructure to manage and run a modeling system based on the algorithms implemented in the open-source numerical models *Weather Research and Forecasting* (WRF) (Skamarock et al. 2001) and *WavewatchIII* (WW3) (Tolman 2009) organized in a workflow (Montella et al. 2015). The management of this complex data acquisition, processing, simulation, post-processing and intercomparison dataflow was provided by FACE-IT workflow engine, available as open source and cloud service. FACE-IT infrastructure is extended in order to support applications related to weather, sea wave conditions, ocean circulation and pollutant transport and diffusion.

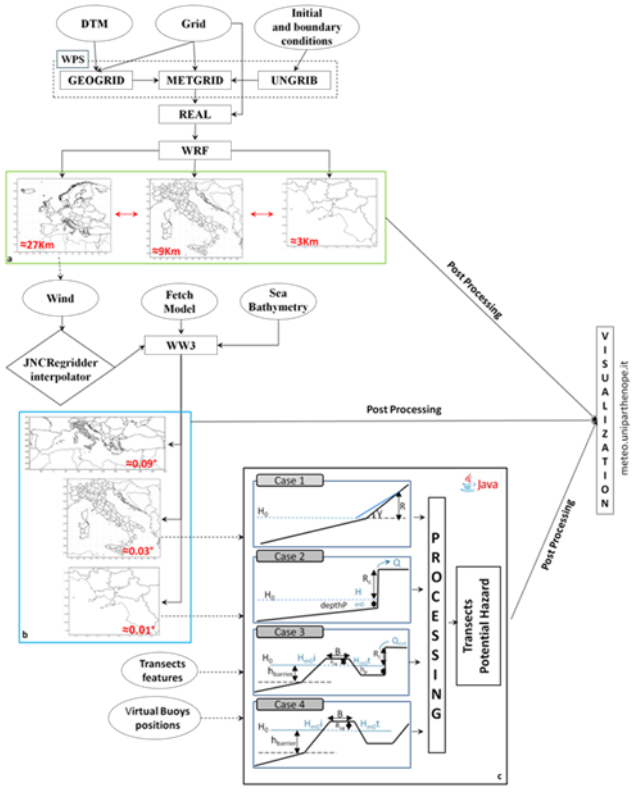

Fig.1 Scientific workflow. The figure shows also WRF (box a) and WW3 (box b) models resolution of each spatial domain. The box c shows the four scenarios actually implemented in the run-up/overtopping model.

This integrated data processing and simulation framework enables: i) the data ingest from geospatial archives; ii) the data regridding, aggregation, and other processing prior to simulation; iii) the leveraging of the high-performance and the cloud computing; iv) the post-processing to produce aggregated yields and ensemble variables needed for statistics and model testing.

The models coupling and the offline grids nesting involved the development of several pre-processing and post-processing software in Java and Python programming languages.

The main workflow tool is the WRF numerical model which gives the atmospheric forcing needed to drive WWIII model for estimating the offshore waves, which is the initial and boundary conditions for the modeling of waves in shallow water and run-up/overtopping calculator software. Wind forcing required to drive WWIII models has been provided by 10-m wind fields obtained using WRF model for all the case studies presented in this paper. The WRF initial and boundary conditions are obtained by the operational Global Forecast System (GFS) model outputs (0.5°x0.5° spatial resolution).

A single computational domain of 300x209 horizontal grid points on Arakawa C-grid staggering and 28 vertical levels has been defined for the WRF model, covering the whole Mediterranean with spatial resolution of about 27 km. The model outputs are generated each 1 hour.

Wave simulations were carried out using the *WaveWatchIII* model (Tolman and Chalikov 2009), a third generation wave model developed at NOAA/NCEP.

The governing equations simulate variations in time and space of wave growth and decay produced by the surface wind, dissipation and bottom friction effects.

Wave propagation is described by:

$$\frac{DN}{Dt} = \frac{S_{lin}+S_{in}+S_{nl}+S_{ds}+S_{db}+S_{bot}}{\sigma} \quad (1)$$

In witch S represent the net effect of sources and sinks for the $N(k,\Theta)$ in which k and Θ are the wavenumber and the direction respectively. The net source term is the sum of a linear input source term (S_{lin}) (Cavaleri et al. 1981), a wind-wave interaction term (S_{in}) (Tolman 1996), a nonlinear wave-wave interactions term S_{nl} (Hasselmann 1985), a dissipation term (S_{ds}) (Tolman 1996), the depth-induced breaking dissipation term (S_{db}) (Battjes and Janssen 1978) and a wave-bottom interactions term in shallow water (S_{bot}) (Hasselmann et al. 1973).

Outputs from the model include gridded fields with the associated significant wave height (H_s), wave direction (Dir_{mn}), mean period (T_m) and the spectral information.

The WW3 grid points close to the coast were used as "*virtual buoys*" (VB) to compute the wave transformation down to the coast, with the final goal of forecasting the run-up and overtopping parameters on the beaches and on the coastal infrastructures.

Different empirical formulas are used to calculate the wave run-up and/or overtopping parameters necessary to estimate the vulnerability for each transect. The approach depends on the coastal morphology (low and sandy beach or high and rocky cliff) and on the possible presence of protection structures (ex. seawalls and breakwaters). Actually the tool considers the following scenarios: i) beach (Mase 1989); ii) vertical or sub-vertical seawall (Allsop et al. 2008); iii) beach with detached breakwater (Hunt 1959, Battjes 1974); iv) seawall with detached breakwater. The present paper is focused on the beach case test.

In the beach case, the algorithm analyzes the hydrodynamic features considering beach-waves interaction to calculate the wave 10% run-up exceedance parameter ($R_{10\%}$), which depends on the incident wave steepness and the geometrical beach characteristics.

The calculations of $R_{10\%}$ ware made on the basis of the deepwater significant wave height (H_0), the corresponding wave length (L_0) (Airy 1841), the mean wave period (T_m) and the beach slope angle (γ), using the general relationship (Mase 1989):

$$\frac{R_{10\%}}{H_0} = a\xi^b \quad (2)$$

In witch $\xi=(\tan\gamma)/(H_0/L_0)^{1/2}$ is the Iribarren parameter (Iribarren et al. 1949). The coefficients *a* and *b* depend on the statistic ($R_{n\%}$) desired and in accord to Mase (1989), their values are 1.70 and 0.71 respectively.

H_0 depends on the relation between the VB ($C_{VB}=L_{VB}/T_m$) and the deep water ($C_0=L_0/T_m=(gT_m)/(2\pi)$) (Shore Protection Manual 1984) wave celerity:

$$H_0 = H_s \frac{C_{VB}}{C_0} \quad (3)$$

In VB the wavelength is equal to $L_{VB}=(2\pi)/k$ in which k is the wavenumber obtained by the Hunt (1979) approximation of the standard dispersion relation (Fenton et al. 1990):

$$(kd)^2 = \left(\frac{\sigma^2 d}{g}\right)^2 + \frac{\left(\frac{\sigma^2 d}{g}\right)}{\sum_{n=1}^{\infty} d_n \left(\frac{\sigma^2 d}{g}\right)^n} \quad (4)$$

In witch the d_n are given by $d_1=0.6666666667$, $d_2=0.3555555556$, $d_3=0.1608465608$, $d_4=0.0632098765$, $d_5=0.0217540484$, $d_6=0.0065407983$ and $\sigma=2\pi/T_m$ is the wave frequency.

The beach slope is dynamically calculated by taking into to account the profile for each coastal transect considered. The extent of flooding and the corresponding hazard level depends on the beach slope and the run-up parameter.

The alert system allows the operational checking monitors hourly for flood hazard the results of the computation for all transect along the coastal area and reports the overcoming of threshold through a service of automated messages to a selected user list. The alert message shows the time and location of the storm and the level of danger to which the citizens and the infrastructure can be potentially exposed.

The system has been implemented in Java using the software component Jython and the CCMMMA openly available web REST API.

2.2 Field dataset

The choice of the dataset to compare with the model simulation results depends on the availability of the observations during the sea storms considered in this paper and by the data spatial distribution in the area interested by the storms.

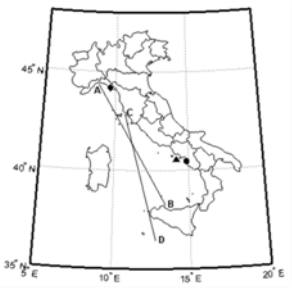

Fig. 2 Map showing the position of the dataset to models testing

In Fig. 2 the AB line depict the ESA Envisat satellite, the CD line depict the OSTM/Jason-2 satellite, the Triangle and circle points are Capri and Salerno (Campania Region) wave buoys respectively, and the rhombus point is the beach camera on Bonassola beach (Ligurian Region).

2.2.1 Buoy measurements

In order to testing the reliability of WW3 model we used the recorded buoy data (SWH, wave period and wave direction) measured in two marine offshore points of interest located in Tyrrhenian sea:

- Buoy 1: a directional waverider buoy (40°32'06''N, 14°11'23''E) installed offshore Capri Island and managed by the Civil Protection Department of the Campania Region.
- Buoy 2: a directional waverider wave buoy (40°27'26.4''N, 14°51'41.16''E) installed and managed by the Provincial Authority in the Bay of Salerno on ~35 meter deep water.

Specifically, the buoys measure the frequency and size of wave energy (known as the spectra) from which significant wave height, dominant wave period, and average wave period are derived. Even the direction of wave propagation is measured.

The choice of these two buoys depends on the availability of data for the sea storms considered in this paper. The data time series are continuous and do not present anomalies related to malfunctions of the buoys. The data are collected every 30 minutes.

The examined case studies were obtained by the buoy 1 in a wave storm from 1 to 3 January 2010, with a maximum value of H_s recorded in-situ of 5.94m at 02/01/2010 19pm (UTM).

The second wave storm was recorded by the Salerno buoy from 9 to 11 February 2016, with a maximum wave height of 3.3m at 10/02/2016 14pm (UTM).

2.2.2 Altimeter data

The altimeter data was obtained from two dataset:

- Dataset 1: The *Ocean Surface Topography Mission* (OSTM/Jason-2) was launched on 20 June 2008. In this case we use the *Interim Geophysical Data Record* (IGDR) data with spatial resolution of 11.2 km (Along) x 5.1 km (Across). The passes (half a revolution of the earth by the satellite from extreme latitude to the opposite extreme latitude) are numbered from 1 to 254 representing a full repeat cycle of the OSTM/Jason-2 ground track. Ascending passes are odd numbered and descending passes are even numbered. After one repeat cycle of 254 passes, OSTM/Jason-2 revisits the same ground-track

within a margin of ±1 km. That means that every location along the OSTM/Jason-2 ground-track is measured every approximately 9.9 days (Dumont et al. 2009).

- Dataset 2: The *Environmental Satellite* (ENVISAT) with *Radar Altimeter 2* (RA-2) was launched on March 2002. The satellite orbit is sun-synchronous at an altitude of 800 km, with an inclination of 98.54°. The selected orbit has a repeat cycle of 35 days and an orbital period of 100.6 min (Benveniste et al. 2002).

The choice of these two satellites depends on the availability of data during the sea storms 1 to 3 January 2010 considered in this paper. The altimeter observations are provided along the satellite tracks, which covered part of the Ligurian and Tyrrhenian seas.

The ESA Envisat dataset is relative to 31 December 2009 between 20:43 UTC and 20:45 UTC (pass. 715, cycle 85) and data coordinates are along the AB line in Fig. 2. The OSTM/JASON2 dataset is relative 31 December 2009 between 04:30 UTC and 04:31 UTC (pass. 44, cycle 55) and the data coordinates are along the CD line in Fig. 2.

2.2.2 Video-camera system and images elaboration

The video monitoring system used in this paper to test the beach flooding model, consists of three cameras allowing almost full coverage of the Bonassola beach (Liguria region, north-western Italy) to monitor the wave motion during the storm event. The three cameras were installed at an elevation of about 13 m above *Mean Sea Level* (MSL) and their view range allowed a complete coverage of the beach since 19 November 2015 until now. Images were acquired with a frame rate of 1 Hz, with automated process of data collection. The images processing is carried out with the software *Beachkeeper plus* (Brignone et al. 2012), based on Matlab algorithm to analyze the images without any a-priori information of the acquisition system itself.

3 Wave model comparisons with buoy measurements

The numerical tests performed regarded two aspects: i) the wave model; ii) the run-up model.

The wave model tests were validated with wave buoy measurements and satellite altimeter data, while the run-up model was validated with the beach video camera system.

The tests were carried out during two sea storm events which interested Italy's western coast (Tyrrhenian and Ligurian Seas): i) the first storm is relative to 1-3 January 2010; ii) the second storm is relative to 9-11 February 2016.

In both cases, the 10m wind fields used to force the wave model ware computed by WRF model on a spatial domain of 300x209x28 grid points and about 27 Km in global horizontal resolution, with a mesh grid centered in Lat=50.36N, Lon=8.96E (Mediterranean Sea).

In order to test WW3 offshore wave model in different spatial resolution, two nested model grid domains were configured : i) 352x485 grid points and 0.03° spatial resolution in latitude (Lat_{min}=36.42N, Lat_{max}=46.98N) and in longitude (Lon_{min}=6.33E, Lon_{max}=20.88E), including the Seas around Italy; ii) 350x200 grid points and 0.01° spatial resolution in latitude (Lat_{min}=39.50N, Lat_{max}=41.49N) and in longitude (Lon_{min}=12.50E, Lon_{max}=15.99E), covered Tyrrhenian Sea.

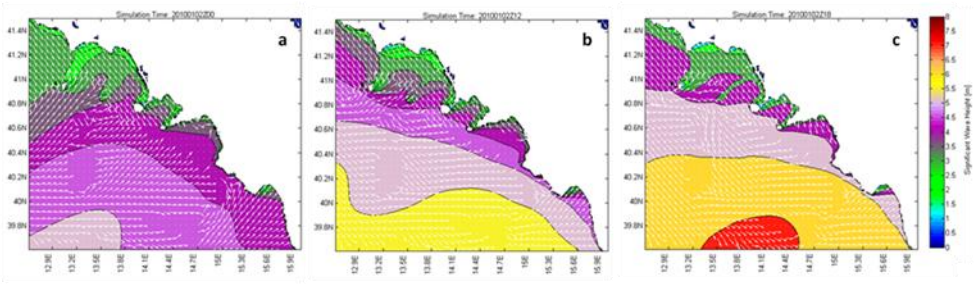

Fig. 3 Significant wave height (color maps) and direction (vector fields) in three moments of sea storm in January 2010. The maps are relative to *WaveWatchIII* model forecast in the time interval: (a) 02/01/2010 at 00:00 UTM; (b) 02/01/2010 at 18:00 UTM; (c) 02/01/2010 at 12:00. Wave height isolines are at 0.5 m intervals

The reliability of WW3 numerical model was assessed in local scale, by comparisons between forecast data of the principal wave parameters (H_s, T_m, Dir_{mn}) and buoy data recorded in Capri (buoy 1) and Salerno (buoy 2). For each simulation the error indices (Mentaschi et al. 2013) were calculated: *Bias* (BI), *Root Mean Square Error* (RMSE), *Scatter Index* (SI), and *Correlation Coefficient* (R). In Fig. 3 the spatial wave simulations relative to first storm have been reported, with reference to the Southern Tyrrhenian Sea, while in Fig. 4 the H_s and T_m time series (recorded and forecasted) have been compared.

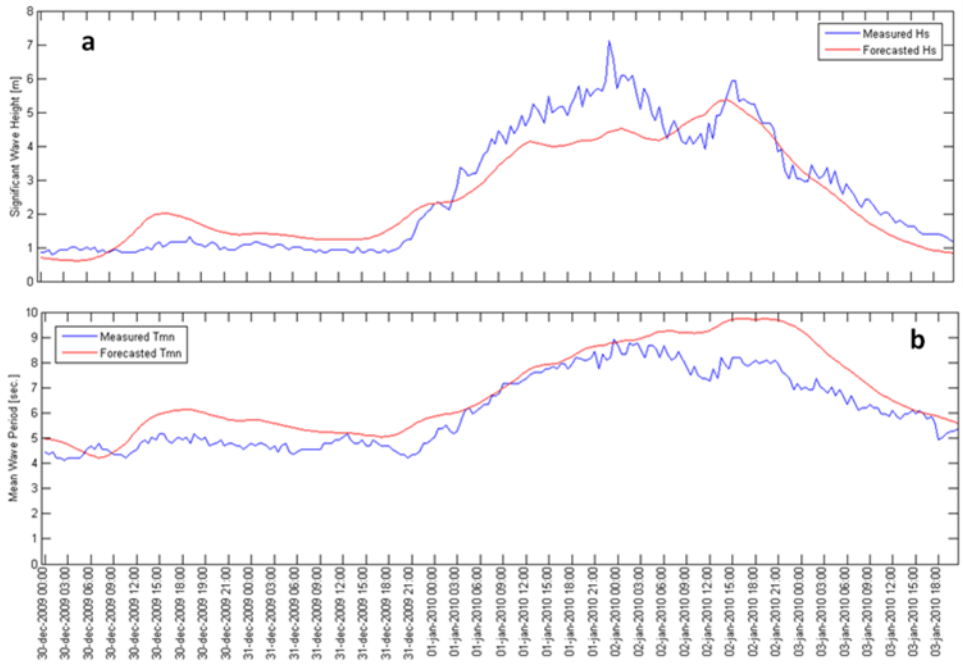

Fig. 4 Significant wave height (H_s) and wave mean period (T_m) forecasted and measured time series. The measured in-situ data has been recorded by Capri buoy. The time series is relative to 30 December-04 January 2010 sea storm

The comparison shows as the significant wave height value is sometimes underestimated by the model, while the wave period is slightly overestimated. This is probably linked with the wave forcing resolution (wind field at 10m MSL) which is not very high for a local scale (we use a 27Km wind fields spatial resolution). Specifically, the meteorological structure, used as forcing, was in general correct, but there was an underestimation of the 10m wind speeds.

With reference to the previous storm, the Fig. 5 shows the scatter plot for the significant wave height (a), the mean wave period (b) and the mean wave direction (c), obtained using data collected from the Capri buoy (x-axes) and the WW3 model results (y-axes). The considered data are related on all the time series.

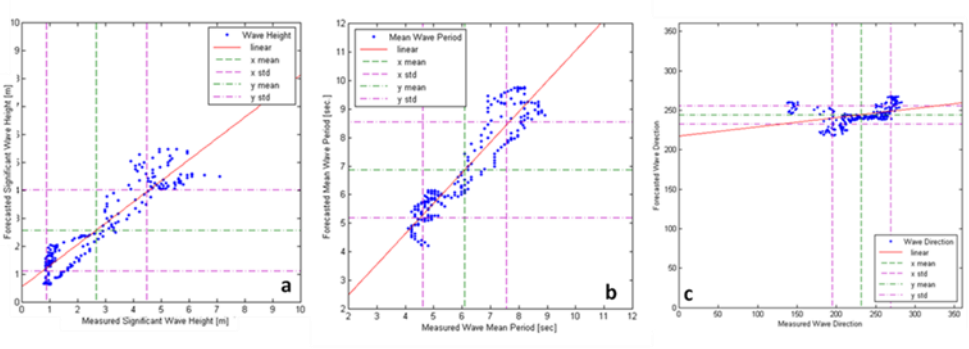

Fig. 5 Probability density scatter plot comparison between forecasted and measured: (a) Significant Wave Height; (b) Mean Wave Period; (c) Mean Wave Direction, during 30 December-04 January 2010 sea storm

The relevant statistical indices obtained by the inter-comparison have been reported in table 1. The correlation coefficient determines the degree to which the measured and forecasted variables are related, and its values are near to 1 for all the parameters. Particularly, the significant wave height have R value equal to 0.9398, the mean wave period have R value equal to 0.9387 and wave direction have R value equal to 0.7232.

Table 1 – Statistical index relating to the comparison between the wave parameters simulated by WW3 model and the Capri buoy dataset during 30 December-04 January 2010 sea storm.

	Correlation Coefficient (R)	**Bias (BI)**	**Scatter Index (SI)**	**Root Mean Square Error (RMSE)**
Significant Wave Height (H_s)	0.9398	-0.0348	21%	0.6660
Mean Wave Period (T_m)	0.9387	0.1281	16%	0.9767
Mean Wave Direction (Dir_{mn})	0.7232	0.0080	8%	19.8146

The scatter index and Bias are normalized with the average observed values. The significant wave height has a negative BI unlike the other two parameters. Negative bias denotes lower model values with respect to buoy observations. The H_s and Dir_{mn} BI value is very close to zero.

The scatter index, defined as the standard deviation of the difference between model and buoy normalized by the observation mean (Bidlot et al. 2002), has a lowest value for the wave direction (8%) and values greater than 15% for H_s (21%) and T_m (16%).

Then, the statistics is satisfactory.

The significant wave height spatial distribution during the second sea storm is reported in Fig. 6. The simulation is relative to WW3 model with ~0.03° spatial resolution.

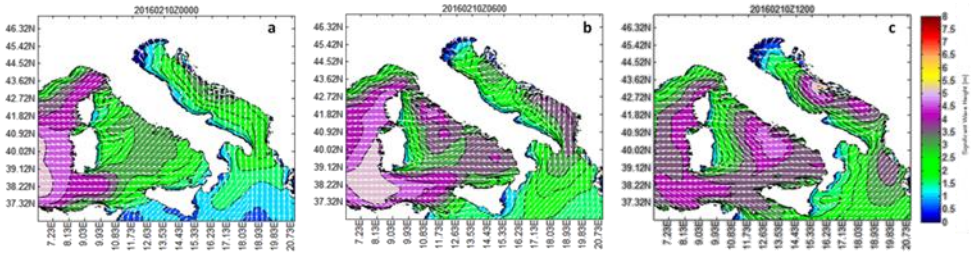

Fig. 6 Significant wave height (color maps) and direction (vector fields) in three moments of sea storm in February 2016. The maps are relative to *WaveWatchIII* model forecast in the time interval: (a) 10/02/2016 at 00:00 UTM; (b) 10/02/2016 at 12:00 UTM; (c) 10/12/2016 at 12:00. Wave height isolines are at 0.5 m intervals

The validation of the simulated results with reference to the second storm is reported in Fig.7-8. The time series (Fig. 7) shows consistent trends for H_s (a) and T_m (b) but the wave period is overestimated by the model for the first two simulation days.

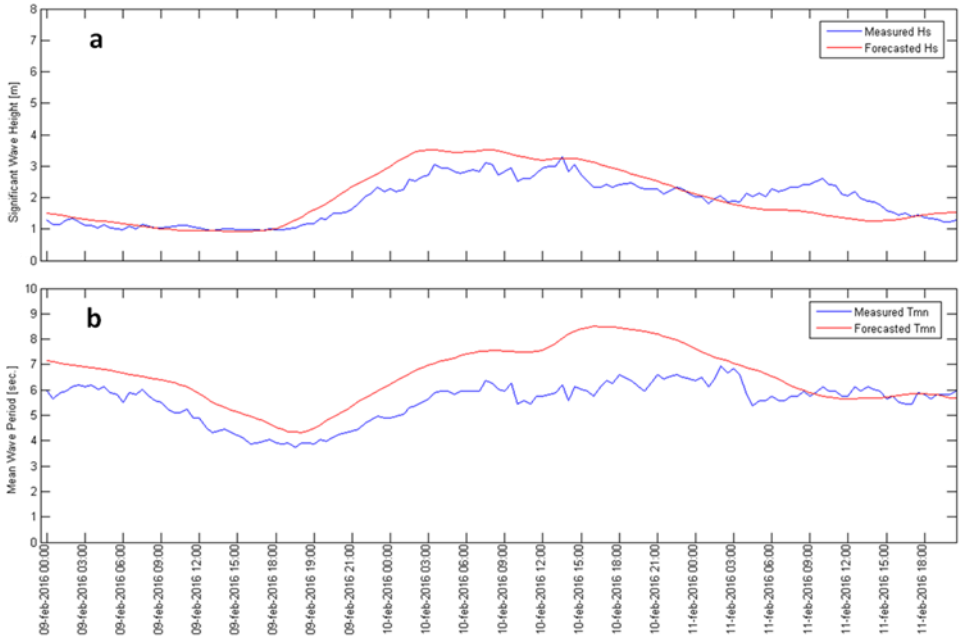

Fig. 7 Significant wave height (H_s) and mean wave period (T_m) time series. The measured in-situ data are recorded by Capri buoy. The time series is relative to 09-11 February 2016 sea storm

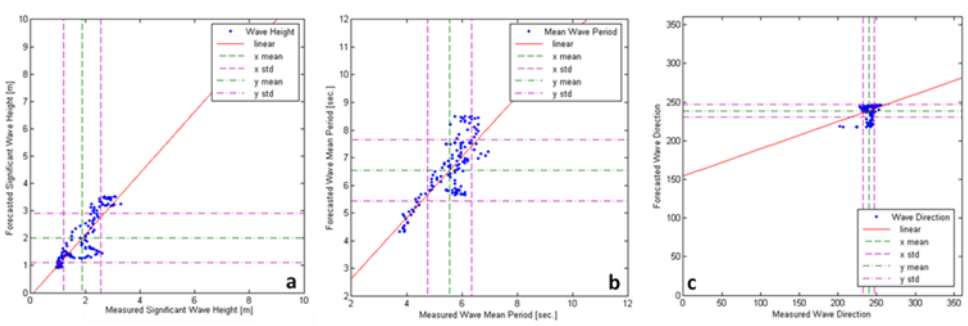

Fig. 8 Probability density scatter plot comparison between forecasted and measured (a) Significant Wave Height (b) Mean Wave Period (c) Mean Wave Direction during 09-11 February 2016 sea storm

In table 2 we show the statistical values obtained by the inter-comparison between the recorded and simulated wave parameters. The H_s has a small mean difference between model and observations (BI equal to 0.0620) with a high data correlation.

The correlation coefficient shows a positive relationship between the measured and forecasted variables in the cases of H_s (0.8609) and T_m (0.7773). Instead, the value of the R index for the wave direction is small (0.3186). The scatter index assume a lowest value for the wave direction (4%) and values greater than 20% for H_s (24%) and T_m (22%).

Table 2 - Statistical parameters to evaluate WW3 model performance respect to Salerno buoy registrations on 09-11 February 2016 sea storm sea storm.

	Correlation Coefficient (R)	**Bias (BI)**	**Scatter Index (SI)**	**Root Mean Square Error (RMSE)**
Significant Wave Height (H_s)	0.8609	0.0620	24%	0.4749
Mean Wave Period (T_m)	0.7773	0.1777	22%	1.2113
Mean Wave Direction (Dir_{mn})	0.3186	-0.0043	4%	9.2427

4 Wave model comparisons with altimeter data

Two satellite orbits cover the initial preliminary phase of sea storm from 1 to 3 January 2010, the ESA Envisat and OSTM/Jason-2. The tracks are along the Ligurian and Tyrrhenian Sea.

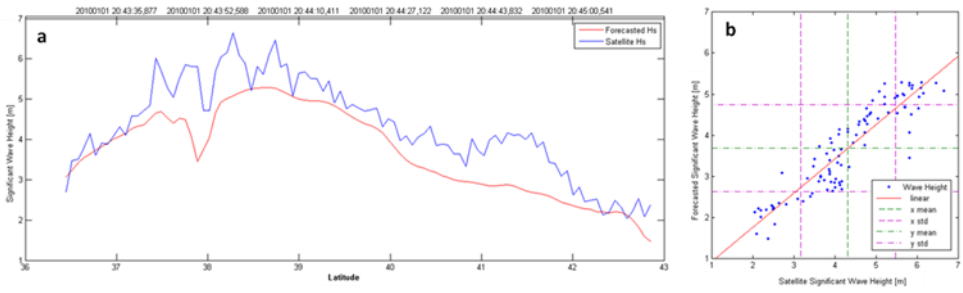

Fig. 9 Matching between WW3 model and altimeter data Envisat pass. 715 cycle 85

The track in figure Fig. 9a corresponds to the passage of Envisat satellite on 31 December 2009 between 20:43 UTC and 20:45 UTC.

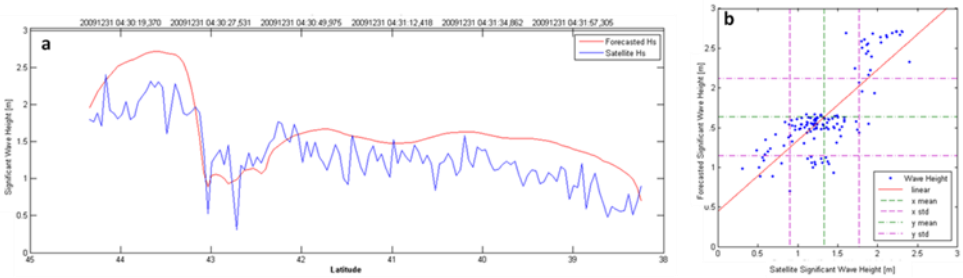

Fig. 10 Matching between WW3 and altimeter data OSTM/Jason-2 pass. 44 cycle 55

The track in figure Fig. 10a corresponds to the passage of OSTM/Jason-2 on 31 December 2009 between 04:30 UTC and 04:31 UTC.

The figures Fig. 9b and Fig. 10b shows the comparison between H_s forecasted and observed for Envisat and OSTM/Jason-2 respectively. Taking this into account, it is comforting to see that while the quality of fitting between model and altimeter may vary, most features of the measured data are reproduced by the model.

Also in this case the statistic indexes give more information about the relation between the two datasets (observed and forecasted).

The table 3 shows, for each satellite, the values of statistical indicators to evaluate WW3 model performances. As you can see, there is a greater correlation (0.9134) between the forecasted significant wave height values and the Envisat satellite observations. The correlation between model and Jason-2 observed significant wave height is 0.7984. In both cases the values of R index are nearest to 1 so, the forecasting simulation are considerate very positive related.

Table 3 - Statistical parameters to evaluate WW3 model performance respect to altimeter data on 09-11 February 2016 sea storm.

	Correlation Coefficient (R)	**Bias (BI)**	**Scatter Index (SI)**	**Root Mean Square Error (RMSE)**
Significant Wave Height – OSTM/Jason2	0.7984	0.2279	30%	0.4239
Significant Wave Height – Envisat	0.9134	-0.1455	18%	0.7834

5 Run-up model comparisons with camera system

In order to improve the reliability of the software that govern the physical wave transport to coast and the compute the run-up on the beach we use a video-monitoring system. Wave rup-up values computed by run-up operational software calculator have been validated by observed wave run-up data recorded by beach camera system. The data were referred to storm from 9 to 11 February 2016.

Test case presented in this work was carried out on Bonassola beach (SP) in the Ligurian Sea coast of Italy.

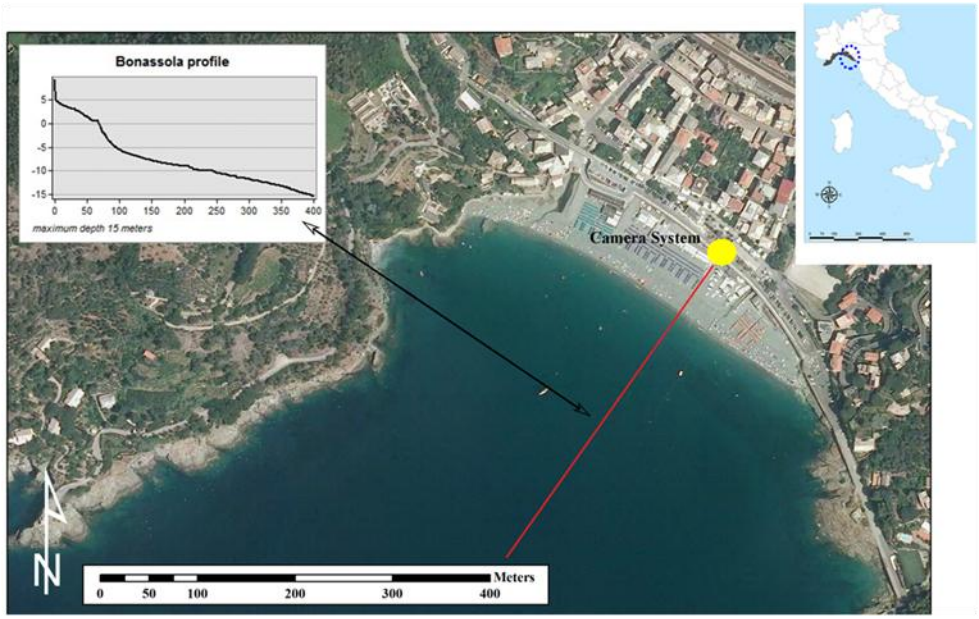

Fig. 11 Bonassola beach. Red line shows the investigated profile and the graph draws morphodynamic features. Yellow circle represents camera system location

This gravel beach has steep and typically concave profiles with slope increasing up the beach face. Cusps are observable along the shore. These features could be associated to the presence of rip currents. Nearshore has a slope approximately 8.3% from the shoreline to 10m water depth and becomes 5.5% at water depth of 10 to 30m (Fig. 11). The offshore beach is composed by sands. To the boundaries, close to the promontories the bedrock outcrops, covered by sea-grasses (*Posidonia Oceanica* and *Cymodocea Nodosa*). The beach is stable and partially protected by wave attack from SE and SW. Video monitoring system was placed in the middle of beach (Fig. 11 yellow circle). Fig. 12 shows the offshore (in the virtual buoy point) wave properties during the sea storm.

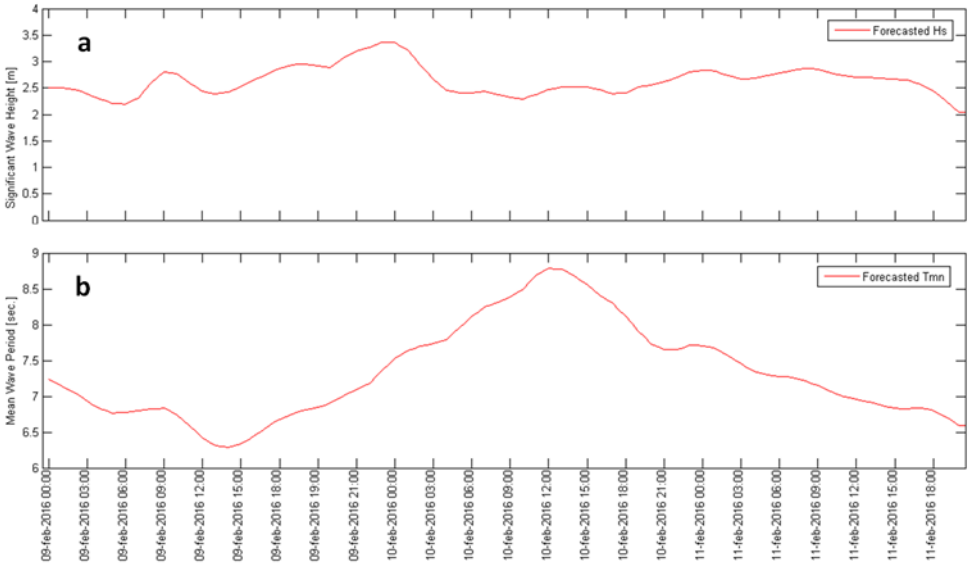

Fig. 12 Forecasted significant wave height (H_s) and mean wave period (T_m) time series, relative to 09-11 February 2016 sea storm on virtual buoy near Bonassola beach

Results were referred to range time from 08:00am to 16:00pm of 10 February 2016.

For the purpose of obtaining the wave run-up line from the geo-referenced video images of the central camera, the technique of the timestack analysis was employed. The timestack is described in the extensive literature on coastal video monitoring (Takewaka e Takashi 2000, Ojeda et al. 2008, Zhang 2008, Kuo et al. 2009). The images for wave run-up measurements were generated on hourly basis along the profile show in Fig. 11. In this work has been evaluated 10% exceedance value ($R_{10\%}$) (McCall et al 2014).

Fig. 13 shown wave run-up excursion recorded by central camera.

First results, from 8:00am to 09:00am, $R_{10\%}$ value was 3.05 meters with maximum excursion around 4.5 meters, while second time step shown 3.31 meters $R_{10\%}$ value with maximum wave run-up value about 4.3 meters. From 10:00am to 11:00am $R_{10\%}$ value was 3.43 meters and maximum value 4.4 meters.

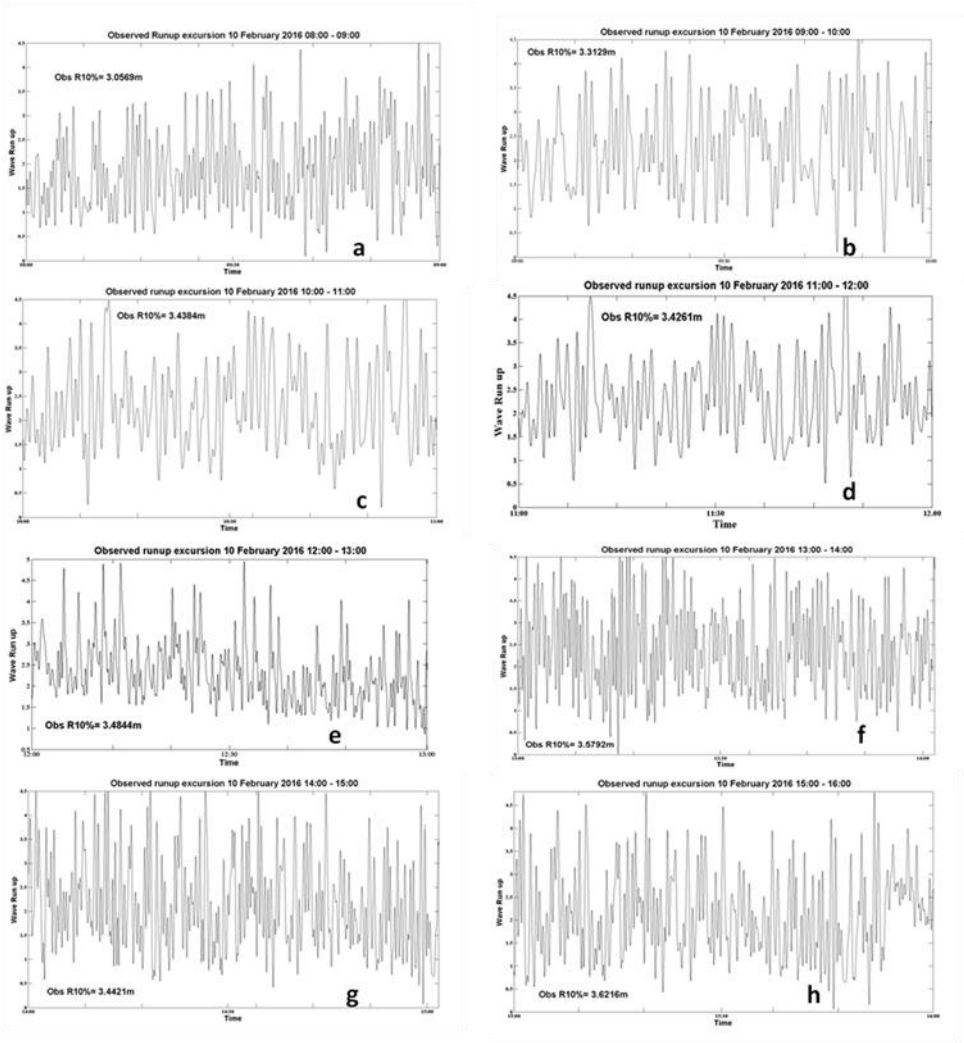

Fig. 13 Wave run-up levels collected using pixel time stacks derived from video data of camera at Bonassola in 10 February 2016 at: (a) 8:00-9:00 UTC; (b) 9:00-10:00 UTC; (c) 10:00-11:00 UTC; (d) 11:00-12:00 UTC; (e) 12:00-13:00 UTC; (f) 13:00-14:00 UTC; (g) 14:00-15:00 UTC; (h) 15:00-16:00 UTC

In Fig. 14 you can observe some beach camera acquisition during the sea storm in Bonassola and a timestack relative to 10/02/2016 08:00 to 09:00 UTC (Fig. 14e).

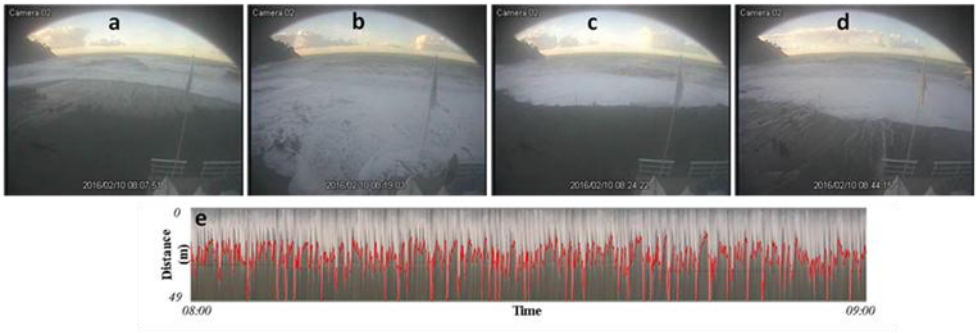

Fig. 14 Camera view refer to investigated profile and Time stack image (shown on bottom) relative to 10/02/2016 08:00 to 09:00 UTC

Fig. 15b shows the time series relative to R10% model forecasted in 10/02/2016 08:00am to 16:00pm.

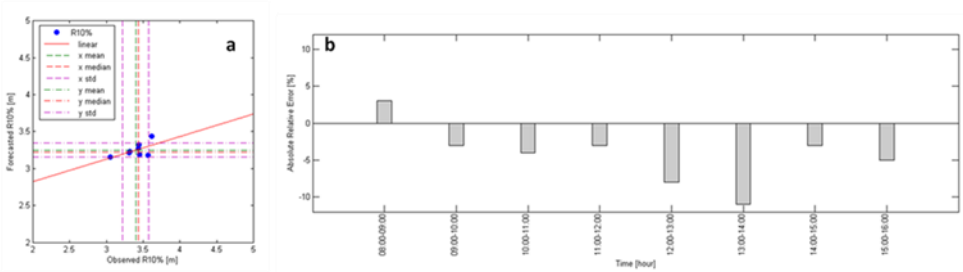

Fig. 15 Comparison between $R_{10\%}$ observed with beach cameras and the same parameter model forecasted. Scatter diagram and data statistic (a) and *Absolute Relative Error* (b). Data are referred to range time from 08:00am to 16:00pm of 10 February 2016

$R_{10\%}$ forecasted values have been compared with $R_{10\%}$ observed values calculated on wave run-up excursions recorded by camera system on Bonassola beach. Following McCall et al. (2014), *Absolute Relative Error* (ARE) was estimated for each hour examined in this work.

$$ARE = \frac{R_{10\%}forecasted - R_{10\%}Observed}{R_{10\%}Observed} \quad (5)$$

Table 4 - $R_{10\%}$ Observed versus $R_{10\%}$ Forecasted and *Absolute Relative Error*

Time (UTC)	$R_{10\%}$ Observed	$R_{10\%}$ Forecasted	ARE
10 February 08:00 - 09:00	3.05	3.16	0.03 (3%)
10 February 09:00 - 10:00	3.31	3.21	-0.03 (-3%)
10 February 10:00 - 11:00	3.43	3.27	-0.04 (-4%)
10 February 11:00 - 12:00	3.42	3.23	-0.05 (-5%)
10 February 12:00 - 13:00	3.45	3.19	-0.08 (-8%)
10 February 13:00 - 14:00	3.57	3.18	-0.11 (-11%)
10 February 14:00 - 15:00	3.44	3.32	-0.03 (-3%)
10 February 15:00 - 16:00	3.62	3.44	-0.05 (-5%)

Results show suitable performance of wave run-up calculator on Bonassola beach. ARE values highlight $R_{10\%}$ forecasted underrated compared with $R_{10\%}$ observed, with maximum difference in elevation around 0.4 meters (ARE 11%). It is worth highlighting that model chain performs well on beach scenarios using Mase formula, indeed RMSE value between observed and forecasted is 0.05 meters.

6 Conclusions and future directions

The focus of this study was the testing and validation of the coastal flooding alert tool during two severe sea storms interested the Italy's east coast in January 2010 and February 2016. The performances evaluation is done separately for the wave forecast model and the beach run-up calculator.

The prediction of intense and small scale events is much more difficult just because of the increased difficulty of a meteorological model to handle strong gradients (Bertotti and Cavaleri 2009). In the open sea this is not a problem but, in small sea areas, the wave propagation depends in practice only on the local meteorological ones.

As the comparison shown, the errors on model wave estimate offshore become very small during the propagation to coast, so the underestimation or overestimation of run-up on the beach are acceptable if we consider the goal of the alert system.

The accurate forecast of sea storms is important for the large impact that the weather-marine extreme events have on the economy, and on the civil and environmental protection. Thus, if coastal manager knows when the sea storm is likely to occur, they can minimize the damages caused by this event.

The methods described in this paper provide a basis for the study of coastal flooding with operational oceanography model instruments. Its provide a valuable management support to local governments and to resorts, which will organize inter-annual activities ensuring the security of citizens and infrastructures overlooking the coast.

Video-monitoring is also used to study the shoreline response to storm events, the evolution of beach dunes with regards to the vegetation, slope variation, dune toe regression etc.

The model results will fill some of the data void regarding coastal flood data in some areas and be useful for production of coastal vulnerability maps and community planning efforts.

Our plans about the presented research program are multifold: i) we will put more effort in the run-up and overtopping modeling providing in a near future an open source and freely community available model for operational coastal areas management leveraging on high performance computation resources as shared/distributed parallel architectures and GPGPUs (Di Lauro et al. 2012) on both on-premises and cloud computing architectures using RAPID GVirtuS middleware (Montella et al. 2011); ii) Improving the modeling capabilities of our run-up/overtopping model in order to support multiple coastal protection structures and related validation analysis; iii) Extending the modeling domain to a wider area with a continuum like approach over the coastline considering the proximal sea/land use and the geological features, matter pattern and granulometry

providing features and publicly available dissemination tools even leveraging on results of ongoing operational similar projects as the Coastal Emergency Risks Assessment, CERA (Dresback et al. 2013); iv) Promote the beach-cam system to a real-time sensor network fully integrated in our operational stack.

Acknowledgement

This work is in part supported by a project funded by the Municipality of Naples and has been extended in methods and scope by the University of Naples "*Parthenope*" and by C.U.G.RI. (*Inter-University Consortium for the Prediction and Prevention of Major Hazards*); in part supported by TESSA ("*TEchnology for the Situational Sea Awareness*") a industrial research project under the National Operative 20 Program "Ricerca & Competitività 2007-2013" of the Italian Ministry for Education, University and Research; in part by the Grant Agreement number: 644312 - RAPID - H2020-ICT-2014/H2020-ICT-2014-1 "Heterogeneous Secure Multi-level Remote Acceleration Service for Low-Power Integrated Systems and Devices"; in part supported by the NSF cyberSEES program award ACI-1331782, the NSF Decision Making Under Uncertainty program award 0951576, and the DOE under contract DE-AC02-06CH11357; in part by the University of Naples Parthenope - Department of Science and Technologies "*Weather/marine extreme event simulation with Galaxy-ES (Earth System) scientific workflow engine and cloud computing tools*" research project and in part by PROMETEO project, funded by the Campania Region. Buoy data were provided by the Civil Protection Department of the Campania Region and Satellite altimeter data by the RADS and by ESA/ESRIN. The Author are grateful to Eng. Mauro Biafore (Regione Campania) and Dr. Jerome Benveniste for support and advice.

References

Airy, G. B. (1841). Tides and waves.

Allsop, W., Bruce, T., Pullen, T. A., & Van der Meer, J. E. N. T. S. J. E. (2008). Direct hazards from wave overtopping-the forgotten aspect of coastal flood risk assessment?.

Battjes, J. A. (1974). Surf similarity. *Coastal Engineering Proceedings*, *1*(14).

Battjes, J. A., & Janssen, J. P. F. M. (1978). Energy loss and set-up due to breaking of random waves. *Coastal Engineering Proceedings*, *1*(16).

Benassai, G., Montuori, A., Migliaccio, M., & Nunziata, F. (2013). Sea wave modeling with X-band COSMO-SkyMed© SAR-derived wind field forcing and applications in coastal vulnerability assessment. *Ocean Science*, *9*(2), 325-341.

Benassai, G., Migliaccio, M., & Montuori, A. (2013). Sea wave numerical simulations with COSMO-SkyMed© SAR data. *Journal of Coastal Research*, *65*(sp1), 660-665.

Benassai, G., Di Paola, G., & Aucelli, P. P. C. (2015). Coastal risk assessment of a micro-tidal littoral plain in response to sea level rise. *Ocean & Coastal Management*, *104*, 22-35.

Benveniste, J., Baker, S., Bombaci, O., Zeli, C., Venditti, P., Zanife, O. Z., ... & Milagro-Perezin, M. P. (2002). Envisat RA-2/MWR Product Handbook. *Frascati, Italy: Eur. Space Agency*, (1.2).

Bertotti, L., & Cavaleri, L. (2009). Wind and wave predictions in the Adriatic Sea. *Journal of Marine Systems*, *78*, S227-S234.

Bidlot, J. R., Holmes, D. J., Wittmann, P. A., Lalbeharry, R., & Chen, H. S. (2002). Intercomparison of the performance of operational ocean wave forecasting systems with buoy data. *Weather and Forecasting*, *17*(2), 287-310.

Brignone, M., Schiaffino, C. F., Isla, F. I., & Ferrari, M. (2012). A system for beach video-monitoring: Beachkeeper plus. *Computers & Geosciences*, *49*, 53-61.

Carratelli, E. P., Dentale, F., & Reale, F. (2006). NUMERICAL PSEUDO–RANDOM SIMULATION OF SAR SEA AND WIND RESPONSE. *Proceedings of SEASAR*.

Carratelli, E. P., Budillon, G., Dentale, F., Napoli, F., Reale, F., & Spulsi, G. (2007). An experience in monitoring and integrating wind and wave data in the Campania Region. *Bollettino di Geofisica Teorica ed Applicata*, *48*(3), 215-226.

Carratelli, E. P., Dentale, F., & Reale, F. (2007). Reconstruction of SAR wave image effects through pseudo random simulation. *ESA SP*, *636*.

Cavaleri, L., & Rizzoli, P. M. (1981). Wind wave prediction in shallow water: Theory and applications. *Journal of Geophysical Research: Oceans*, *86*(C11), 10961-10973.

Di Lauro, R., Giannone, F., Ambrosio, L., & Montella, R. (2012, July). Virtualizing general purpose GPUs for high performance cloud computing: an application to a fluid simulator. In *2012 IEEE 10th International Symposium on Parallel and Distributed Processing with Applications* (pp. 863-864). IEEE.

Dumont, J. P., Rosmorduc, V., Picot, N., Desai, S., Bonekamp, H., Figa, J., ... & Scharroo, R. (2009). OSTM/Jason-2 products handbook. *CNES: SALP-MU-M-OP-15815-CN, EUMETSAT: EUM/OPS-JAS/MAN/08/0041, JPL: OSTM-29-1237, NOAA/NESDIS: Polar Series/OSTM J*, *400*(1).

Dresback, K.M., J.G. Fleming, B.O. Blanton, C. Kaiser, J.J. Gourley, E.M. Tromble, R.A. Luettich, R.L. Kolar, Y. Hong, S. Van Cooten, H.J. Vergara, Z.L. Flamig, H.M. Lander, K.E.

Kelleher, K.L. Nemunaitis-Monroe, "Skill Assessment of a Real-Time Forecast System Utilizing a Coupled Hydrologic and Coastal Hydrodynamic Model During Hurricane Irene (2011)," Continental Shelf Research, 71, 78-94, 2013.

Fenton, J. D., & McKee, W. D. (1990). On calculating the lengths of water waves. *Coastal Engineering*, *14*(6), 499-513.

Foster, I., Elliott, J. W., Jones, J., & Montella, R. (2013, December). FACE-IT: Framework to Advance Climate, Economics, and Impact Investigations with Information Technology. In *AGU Fall Meeting Abstracts* (Vol. 1, p. 1618).

Giarrusso, C. C., Carratelli, E. P., & Spulsi, G. (1999). Assessment Methods for Sea-RelatedHazards in Coastal Areas. *Natural Hazards*, *20*(2-3), 295-309.

Giunta, G., Montella, R., Mariani, P., & Riccio, A. (2005). Modeling and computational issues for air/water quality problems: A grid computing approach. *Nuovo Cimento C Geophysics Space Physics C*, *28*, 215.

Hasselmann, K., Barnett, T. P., Bouws, E., Carlson, H., Cartwright, D. E., Enke, K., ... & Meerburg, A. (1973). *Measurements of wind-wave growth and swell decay during the Joint North Sea Wave Project (JONSWAP)*. Deutches Hydrographisches Institut.

Hasselmann, S., Hasselmann, K., Allender, J. H., & Barnett, T. P. (1985). Computations and parameterizations of the nonlinear energy transfer in a gravity-wave specturm. Part II: Parameterizations of the nonlinear energy transfer for application in wave models. *Journal of Physical Oceanography*, *15*(11), 1378-1391.

Hunt, I. A. (1959). Design of sea-walls and breakwaters. *Transactions of the American Society of Civil Engineers*, *126*(4), 542-570.

Hunt, J. N. (1979). Direct solution of wave dispersion equation. *Journal of the Waterway, Port, Coastal and Ocean Division*, *105*(4), 457-459.

Iribarren Cavanilles, R., & Casto Nogales, M. (1949). *Protection des ports*. PIANC.

Kuo, C. A., Hwung, H. H., & Chien, C. H. (2009). Using time-stack overlooking images to separate incident and reflected waves in wave flume. *Wave Motion*, *46*(3), 189-199.

Manual, S. P. (1984). Coastal Engineering Research Center. *Department of the Army, Waterways Experiment Station*, *1*.

Mentaschi, L., Besio, G., Cassola, F., & Mazzino, A. (2013). Developing and validating a forecast/hindcast system for the Mediterranean Sea. *Journal of Coastal Research*, *65*(sp2), 1551-1556.

Mase, H. (1989). Random wave runup height on gentle slope. *Journal of Waterway, Port, Coastal, and Ocean Engineering*, *115*(5), 649-661.

McCall, R. T., Masselink, G., Poate, T. G., Roelvink, J. A., Almeida, L. P., Davidson, M., & Russell, P. E. (2014). Modelling storm hydrodynamics on gravel beaches with XBeach-G. *Coastal Engineering*, *91*, 231-250.

Mendoza, E. T., & Jimenez, J. A. (2004). Factors controlling vulnerability to storm impacts along the Catalonian coast. In *COASTAL ENGINEERING CONFERENCE* (Vol. 29, No. 3, p. 3087). ASCE AMERICAN SOCIETY OF CIVIL ENGINEERS.

Montella, R., Giunta, G., & Riccio, A. (2007, June). Using grid computing based components in on demand environmental data delivery. In *Proceedings of the second workshop on Use of P2P, GRID and agents for the development of content networks* (pp. 81-86). ACM.

Montella, R., Coviello, G., Giunta, G., Laccetti, G., Isaila, F., & Blas, J. G. (2011, September). A general-purpose virtualization service for HPC on cloud computing: an application to GPUs. In *International Conference on Parallel Processing and Applied Mathematics* (pp. 740-749). Springer Berlin Heidelberg.

Montella, R., Kelly, D., Xiong, W., Brizius, A., Elliott, J., Madduri, R., ... & Zhang, M. (2015). FACE-IT: A science gateway for food security research. *Concurrency and Computation: Practice and Experience*, *27*(16), 4423-4436.

Ojeda, E., Ruessink, B. G., & Guillen, J. (2008). Morphodynamic response of a two-barred beach to a shoreface nourishment. *Coastal Engineering*, *55*(12), 1185-1196.

Pham, Q., Malik, T., Foster, I. T., Di Lauro, R., & Montella, R. (2012, June). SOLE: Linking Research Papers with Science Objects. In *IPAW* (pp. 203-208).

Reale, F., Dentale, F., Carratelli, E. P., & Torrisi, L. (2013). Remote sensing of small-scale storm variations in coastal seas. *Journal of Coastal Research*, *30*(1), 130-141.

Sartini, L., Besio, G., Dentale, F., & Reale, F. Wave Hindcast Resolution Reliability for Extreme Analysis.

Skamarock, W. C., Klemp, J. B., & Dudhia, J. (2001). Prototypes for the WRF (Weather Research and Forecasting) model. In *Preprints, Ninth Conf. Mesoscale Processes, J11–J15, Amer. Meteorol. Soc., Fort Lauderdale, FL*.

Takewaka, S., & Nakamura, T. (2001). Surf zone imaging with a moored video system. In *COASTAL ENGINEERING CONFERENCE* (Vol. 2, pp. 1211-1216). ASCE AMERICAN SOCIETY OF CIVIL ENGINEERS.

Tolman, H. L., & Chalikov, D. (1996). Source terms in a third-generation wind wave model. *Journal of Physical Oceanography*, *26*(11), 2497-2518.

Tolman, H. L. (2009). User manual and system documentation of WAVEWATCH III TM version 3.14. *Technical note, MMAB Contribution*, *276*.

Zhang, S., & Zhang, C. (2008, May). Application of ridgelet transform to wave direction estimation. In *Image and Signal Processing, 2008. CISP'08. Congress on* (Vol. 2, pp. 690-693). IEEE.